NAIST-IS-DD1761027

Doctoral Dissertation

Design and performance analysis of a suboptimal OFDM receiver for partial time-domain loss scenarios

Chengbo Liu

December 4, 2020

Graduate School of Information Science
Nara Institute of Science and Technology

A Doctoral Dissertation
submitted to Graduate School of Information Science,
Nara Institute of Science and Technology
in partial fulfillment of the requirements for the degree of
Doctor of ENGINEERING

Chengbo Liu

Thesis Committee:

Professor Minoru Okada	(Supervisor)
Professor Kenji Sugimoto	(Co-supervisor)
Associate Professor Takeshi Higashino	(Co-supervisor)
Assistant Professor Duong Quang Thang	(Co-supervisor)
Assistant Professor Na Chen	(Co-supervisor)

Design and performance analysis of a suboptimal OFDM receiver for partial time-domain loss scenarios*

Chengbo Liu

Abstract

Orthogonal Frequency Division Multiplexing (OFDM) has been utilized for many applications such as High Definition Television (HDTV), Wireless Local Area Network (WLAN), 4G, and 5G systems. It has high spectral efficiency and high tolerance to the multipath fading and Impulsive Noise (IN).

However, the transmitted OFDM symbols are damaged due to obstacles and IN in some industrial scenarios (e.g., manufacturing and automatic factories). To recover the damaged signal due to obstacles such as metallic pillars, the OFDM system with Suboptimal Maximum Likelihood sequence estimation (OFDM-SML) utilizes the SML algorithm to reconstruct the original signal with an acceptable complexity. The simulated results show that OFDM-SML can obtain better BER performance than the conventional OFDM system in the AWGN channel even when the half time-domain signal is missing. On the other hand, OFDM-SML with ZF and MMSE can further improve the BER performance of the conventional OFDM when the partial time-domain signal is missing in the WLAN channel. Furthermore, OFDM-SML with MMSE has better BER performance than OFDM-SML with ZF in the WLAN channel when 1/8, 1/4, and 1/2 time-domain signals are missing.

Besides obstacles, the impact of the IN cannot be neglected when the energy of the IN is tremendous. Blanking is a simple method to improve the performance when IN is taken into account in the system. However, this method is sensitive

*Doctoral Dissertation, Graduate School of Information Science,
Nara Institute of Science and Technology, NAIST-IS-DD1761027, December 4, 2020.

to the threshold; namely, it degrades the performance when the useful signal is mistaken as the IN. Therefore, we propose the system which is called OFDM with Suboptimal Maximum Likelihood sequence estimation and Blanking (OFDM-SMLB), to improve the performance of the conventional OFDM using a blanking scheme with an acceptable and flexible complexity. Here OFDM-SMLB utilizes Constant False Alarm Rate (CFAR) to obtain the threshold. The simulated results show that the proposed system can achieve lower BER in the worse case (i.e., high probability of IN occurrence and high IN power).

Keywords:

OFDM system, signal recovery, blanking, impulsive noise

Contents

List of Figures

List of Tables

1 Introduction

1.1 Background

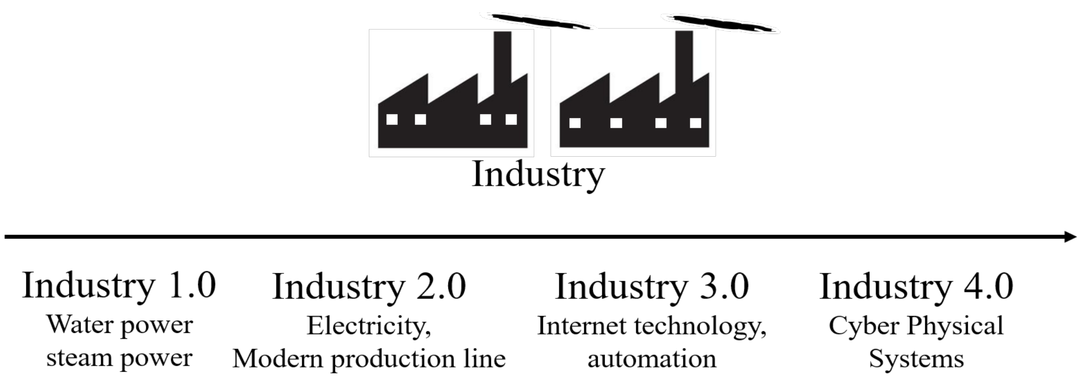

Figure 1.1: Industrial revolution

With the more and more new devices and technologies invented, the fourth revolution (Industrial 4.0) is the ongoing transformation of the modern production line with intelligent technology [1]. Back to the first industrial revolution, it can be called "a qualitative leap". At that time, it was still in pure hand production under the low-efficient, unsafety circumstances. However, when the steam engine was invented, many thoughts and ideas were utilized in many fields such as industry. The machines composed of water and steam power were produced to replace the hand production. After decades of years, the machines based on electricity were created to increase labor production efficiency with the rapid development of technology. This period was the second industrial revolution. At the end of the 20th century, the third revolution (also called the digital revolution) started since communication and Internet technology had significant progress. The timeline of the industrial revolution is shown in Figure 1.1. Nowadays, severe problems such as the vast amount of data volume and the burden of the large number of devices connected to the Internet force us to enter the next industrial transformation from digitalization to intelligence [2].

Industry 4.0 provides manufacturing digitization, optimization in smart factory, human-machine, machine-machine interaction and so on [3, 4]. One of the closest attention is the intelligent manufacturing in the smart factory [5] since it can exponentially increase the efficiency of the production line and create relative job opportunities such as engineering from economic sustainability [6]. In intelligent manufacturing scenarios, mobile robots such as Automated Guided Vehicles (AGV) are utilized to transport the products from one place to another. Generally, AGV has two types of routine line plans: 1) fixed routine and 2) free routine. In the first case, AGV follows the predetermined path-map to fulfill the task. In the second case, AGV can achieve free mobile by current positioning systems (e.g., laser guided vehicles). Both cases should have stable and reliable wireless communication. Wireless Local Area Networks (WLAN) [7] is utilized to provide such wireless communication. However, the received signals may be damaged due to metallic pillars and machines in the industrial environment [8] such as steel works factory, which results in incidents including malfunctioning robots that sometimes hurt people. On the other hand, the occurrence of Impulsive Noise (IN) due to the monitoring applications, ignitions of mobile vehicles [9, 10] leads to an increase of Bit Error Rate (BER). It may cause the problem of connectivity reliability and grow the transmission latency in the event of packet loss [11] in the harsh industrial environment [12, 13], which requires low latency and high reliability [14, 15]. Therefore, we focus on solving two situations in this paper:

1) Damaged signal caused by metallic pillars and machines

2) Impulsive noise.

Orthogonal Frequency Division Multiplexing (OFDM) [16], which is a unique Frequency Division Multiplexing (FDM) [17], is widely utilized in many applications such as WLAN, ISDB-T [18] and 5G [19] - [22]. Figure 1.2 shows the structure of the OFDM system. The input bits are mapped by modulation, such as M-QAM, and passed through the Inverse Fast Fourier Transform (IFFT). Thus, the samples with Guard Interval (GI) insertion are transmitted via D/A over

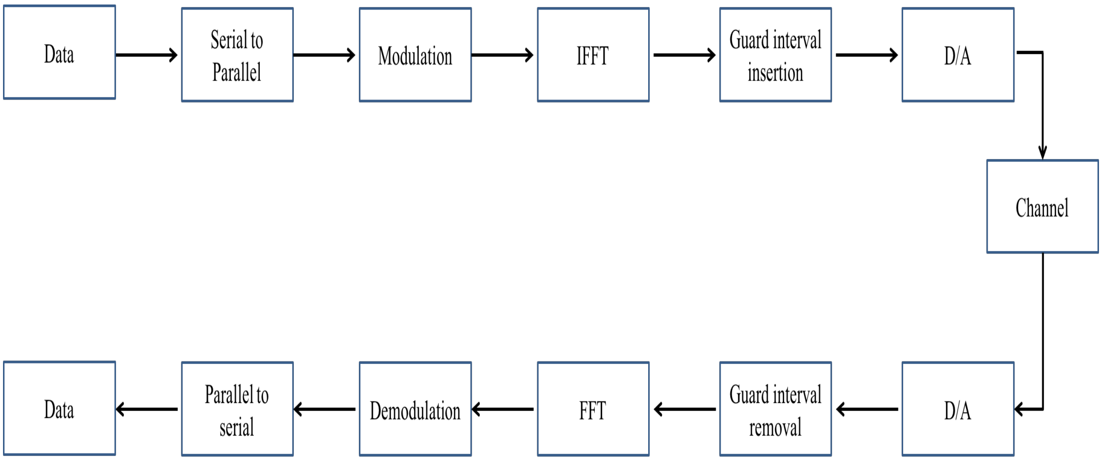

Figure 1.2: Structure of OFDM

the multipath channel. After A/D converter, the symbols remove GI and pass through Fast Fourier Transform (FFT). Finally, the symbols are demodulated to the original data.

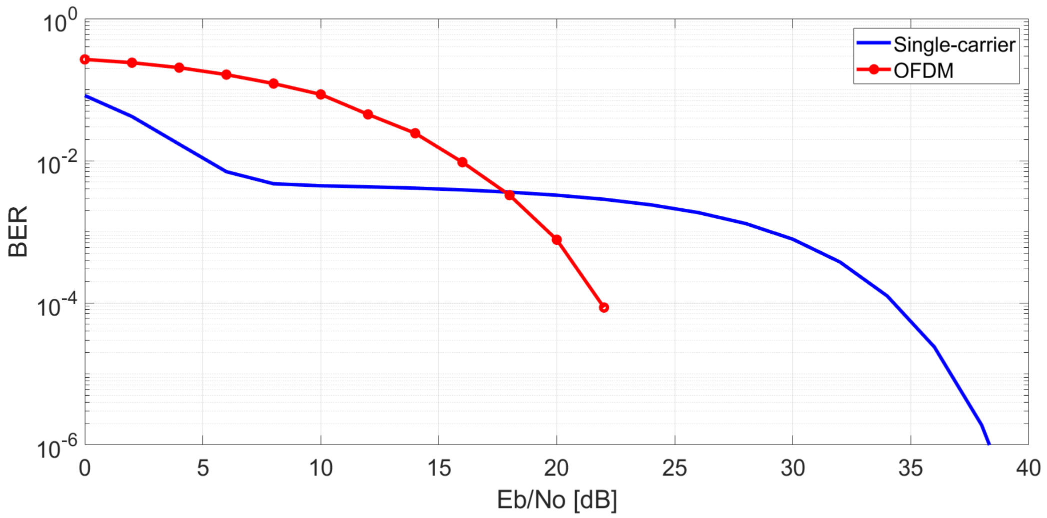

Figure 1.3: BER performance of the single-carrier system and OFDM system using BPSK modulation with $N = 128$ when $q = 0.01$ and $\alpha = 1000$.

OFDM has many advantages compared to that of single-carrier systems. It can increase bandwidth efficiency (BWE) for a given bandwidth due to subcarriers overlapped. Thus, it can eliminate the inter-symbol interference (ISI) due to the Cyclic Prefix (CP). Besides, OFDM has high robustness to frequency selective fading and mitigates the impact of the IN because OFDM can utilize FFT to spread the energy to all the subcarriers. Figure 1.3 shows the BER performance of the OFDM system and the single-carrier system. Here N is the number of subcarriers, q is the probability of IN occurrence, and α is the variance ratio of IN to background noise. Explicitly, the OFDM system can obtain better BER performance than the single-carrier system when Eb/No >= 18dB. However, it turns out to degrade the performance of the system when IN is extensive [23].

1.2 Contributions of this thesis

In this thesis, we utilize OFDM-SML to recover the damaged signal which is partially blocked by obstacles over the fading channel model in the industrial environment. The simulated results show that OFDM-SML can much improve the BER performance assuming that the channel information is correctly detected when the half-time domain symbols are missing in the AWGN channel. In addition, OFDM-SML has more ability to improve the performance with more symbols are missing in the fading channel. For example, OFDM-SML with MMSE can have the best BER performance when 1/8, 1/4 and 1/2 time-domain symbols are missing. Besides OFDM-SML with MMSE, OFDM-SML with ZF also improves the performance of the conventional OFDM systems when 1/2 time-domain symbols are missing.

On the other hand, we propose the OFDM receiver utilizing the combination of Suboptimal MLSE and Blanking (OFDM-SMLB) to mitigate the impact of the IN with an acceptable complexity. Here the proposed system utilizes Constant False Alarm Rate (CFAR) to obtain the location of the IN by distinguishing the mixed signal, including transmitted signal, background noise, and the IN term. Eventually, SML is utilized in the frequency domain to reconstruct the signal after blanking the time-domain signal. The simulated results show that the proposed system performs better than the conventional OFDM with blanking when α is extensive in both non-fading and fading channel models.

1.3 Organization

The paper is organized as follows. Chapter 2 describes OFDM-SML in detail as well as simulated results. In Chapter 3, OFDM-SMLB is presented, and relative simulated results are also introduced. Chapter 4 makes an overall conclusion and discusses future research.

2 OFDM-SML

2.1 Introduction

Smart factory in Industry 4.0 is rapidly developing to solve the labor shortage and economic cost problems. However, the received signals in the OFDM systems may be damaged due to metallic pillars and machines in the harsh industrial environment such as steel works factory, manufacturing and automatic factories. The authors have proposed different methods to solve the problem.

Automatic Repeat Request (ARQ) is the traditional method to cope with signal loss. When the transmitter receives the acknowledgment, it stands for correctly receiving the signal. Otherwise, re-send the signal until the sender receives an acknowledgment. However, the additional cost caused by retransmission is increased, and it is more wasteful for partial signal loss due to metallic pillars and machines. Ref. [24] proposed the Partial Packet Recovery (PPR) to reduce ARQ cost. PPR only retransmits the partial signal which is believed to happen errors. There are two steps in the PPR method: 1) Utilize software to determine which part of the signal is in errors, and 2) Re-send this part of the signal. In our method, we directly reconstruct the damaged signal at the receiver without retransmission.

On the other hand, the adaptive bit loading [25, 26] is utilized to transmit the data on the subcarriers with high SNRs to avoid destroying the signal. However, the feedback at the transmitter limits the loading efficiency and increases the complexity.

The oversampled OFDM with Cyclic Prefix (CP-OFDM) using iterative methods [27,28] has been proposed to recover the damaged signal in the simple channel model, such as the Rayleigh channel, at the cost of complexity. As a matter of fact, the received partial signal has destroyed the orthogonality of the received

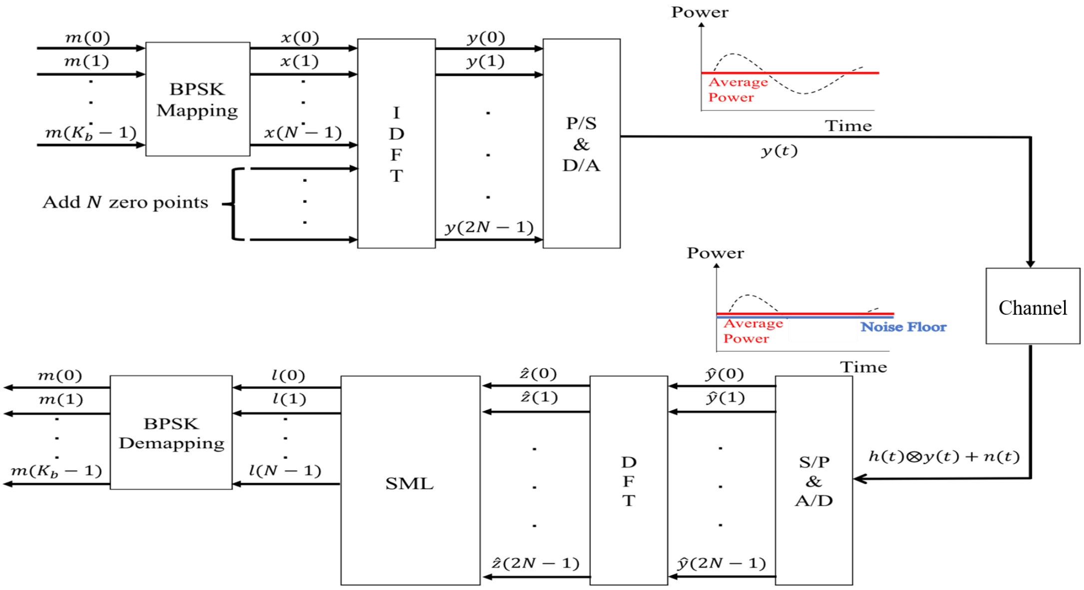

Figure 2.1: Structure of OFDM-SML using BPSK modulation.

signal, and the direct demodulation cannot obtain good performance. Suboptimal Maximum Likelihood sequence estimation (SML) has been proposed in Ref. [29] to improve the performance of OFDM. Therefore, the combination of oversampled OFDM and SML can improve the performance with an acceptable complexity.

2.2 System Model

Figure 2.1 describes the structure of OFDM-SML when some time-domain symbols are missing. Assume that K_b data bits of each symbol are transmitted using N subcarriers. The data bits $x(i)$ mapped by BPSK pad with N zero amplitude points for oversampling at the transmitter. After Inverse Discrete Fourier Transform (IDFT), the output of IDFT is

$$y(k) = \frac{1}{\sqrt{2N}} \sum_{i=0}^{N-1} x(i) e^{\frac{j2\pi ik}{2N}}, k \in [0, \ldots, 2N-1]. \tag{2.1}$$

CP, which is the kind of GI, is added to remove the ISI due to multipath. Thus the time-domain symbols are transmitted via Parallel-to-Serial (P/S) and Digital-to-Analog (D/A) converter over the channel. Here, the impulse response is,

$$h(t) = \sum_{i=1}^{L_p} a_i(t) e^{-j\theta_i(t)} \delta(t - \tau_i), \tag{2.2}$$

with $t \in [0, T + T_{cp}]$. Note that T is the length of the OFDM symbol and T_{cp} is the length of the CP. L_p is the number of the multiple paths where the path has the attenuation $a_i(t)$, phase rotation $\theta_i(t)$, and delay τ_i.

At the receiver, the signal is expressed as

$$\begin{aligned} \hat{y}(t) &= h(t) \otimes y(t) + n(t) \\ &= \sum_{i=1}^{L_p} a_i(t) e^{-j\theta_i(t)} y(t - \tau_n) + n(t), \end{aligned} \tag{2.3}$$

where the $n(t)$ is the complex AWGN noise. Note that some values of the $y(t)$ are set to be zero due to some time-domain symbols blocked by metallic pillars and machines etc.

After S/P and A/D, the discrete samples $\hat{y}(k)$ are represented as

$$\begin{aligned} \hat{y}(k) &= y(k) + n(k) \\ &= \sum_{i=1}^{L_p} a_i e^{-j\theta_i} \sum_{m=0}^{N-1} x(m) e^{\frac{j2\pi m(k - N_{\tau_i})}{2N}} + n(k), \end{aligned} \tag{2.4}$$

with $k \in [0, \dots, 2N-1]$. Assume that a_i and θ_i of each path are constant during the whole OFDM symbol. Here $n(k)$ is the discrete samples of the complex AWGN noise and some values of $y(k)$ are zero. N_{τ_i} is the duration corresponding to the delay τ_i.

After DFT, the $2N$ received samples, $\hat{y}(k)$ yield $\hat{\mathbf{Z}}$=$[\hat{z}(0), \dots, \hat{z}(2N-1)]$ which are represented as

$$\begin{aligned} \hat{z}(l) &= \frac{1}{\sqrt{2N}} \sum_{k=0}^{2N-1} \hat{y}(k) e^{\frac{-j2\pi lk}{2N}} \\ &= \frac{1}{2N} \sum_{k=0}^{2N-1} \left(\sum_{i=1}^{L_p} a_i e^{-j\theta_i} \times \sum_{m=0}^{N-1} x(m) e^{\frac{j2\pi m(k - N_{\tau_i})}{2N}} + n(k) \right) e^{\frac{-j2\pi lk}{2N}}. \end{aligned} \tag{2.5}$$

On the other hand, the Zero Forcing (ZF) equalization and Minimum Mean Square Error (MMSE) equalization are utilized to suppress the impact of the channel. Assume that the channel information is perfectly detected; therefore, the Frequency Impulse Response (FIR) of the channel is expressed as,

$$\begin{aligned} H(k) &= \sum_{l=0}^{2N-1} h(l) e^{\frac{-j2\pi lk}{2N}} \\ &= \sum_{l=0}^{2N-1} \sum_{i=1}^{L_p} a_i e^{-j\theta_i} e^{\frac{-j2\pi l N_{\tau_i}}{2N}}. \end{aligned} \tag{2.6}$$

The ZF equalization of the channel is expressed as,

$$H_{ZF}(k) = \frac{1}{H(k)}. \tag{2.7}$$

The MMSE equalization of the channel is expressed as,

$$H_{MMSE}(k) = \frac{H(k)^*}{\mid H(k) \mid^2 + N_0}, \tag{2.8}$$

where $\left[\cdot\right]^*$ is the conjugate of the value, $\mid \cdot \mid$ stands for the absolute value, and N_0 expresses the power of the AWGN noise.

Therefore, the output of the received symbols via equalization is

$$l(k) = \hat{z}(k) \times H(k), \tag{2.9}$$

where $H(k)$ expresses H_{ZF} or H_{MMSE} depending on the ZF or MMSE equalization. Finally, the damaged symbols can be recovered using SML and demapped by BPSK.

2.3 Signal Recovery Method

Since the received symbols $\hat{y}(t)$ have lost their orthogonality due to partial signal missing, the samples $\hat{z}(k)$ contain the Inter-Carrier Interference (ICI) component which cannot be demodulated independently by each subcarrier.

In this case, we can utilize the Maximum Likelihood Sequence Estimation (MLSE) to demodulate the received symbols. Here MLSE can be represented as

$$\hat{\mathbf{X}} = \arg\min |\hat{\mathbf{Z}} - \mathbf{H_v} \times \hat{\mathbf{X}}|^2, \tag{2.10}$$

with $\mathbf{H_v}$=$[H(0),\ldots,H(2N-1)]^T$, $\hat{\mathbf{X}}_{N\times 1}$=$[\hat{x}(0),\ldots,\hat{x}(N-1)]^T$. Note that $\hat{x}(i)$ belongs to $\{-1,1\}$ and $i=0,1,\ldots,N-1$. The MLSE compares all possible values with the received signals to achieve a good BER performance at the cost of the computational complexity, which increases exponentially as N^P with the number of subcarriers N and the number of constellation subsets of $\{-1,1\}$, P.

SML can reduce the complexity of the MLSE with an acceptable BER performance by removing some candidates depending on the Euclidian distances between received signals and all possible values in every iteration. Its complexity increases linearly as MP with the number of the candidates and the number of constellation subsets of $\{-1,1\}, P$ for BPSK. There is a simple explanation of OFDM-SML below.

Define $\hat{\mathbf{X}}^{(i)(j)}$ as the jth candidate constellation points of the ith iteration process. Assume that P is the number of constellation subset of $\{-1,1\}$. Firstly, the number of the initial candidate constellation points is U, namely, $\hat{\mathbf{X}}^{(1)(u)}$ $=[\hat{x}(0),\ldots,\hat{x}(U-1),\ldots,0]$ with $\hat{x}(k)\in\{-1,1\}$ and $k\in[0,\ldots,U-1]$. Therefore, P^U kinds of $\hat{\mathbf{X}}^{(1)(u)}$ are utilized to calculate the Euclidian distances in the first iteration. $\mathbf{Z}_u^{(1)}=[z_u^{(1)}(0),\ldots,z_u^{(1)}(2N-1)]$ are presented as

$$\mathbf{Z}_u^{(1)}=\mathbf{H_v}\times\hat{\mathbf{X}}^{(1)(u)} \tag{2.11}$$

with $u\in[1,\ldots,P^U]$.

Therefore, the Euclidian distances $d_u^{(1)}$ between $\mathbf{Z}_u^{(1)}$ and the received samples $\hat{\mathbf{Z}}$ are evaluated as

$$d_u^{(1)}=\left(\sum_{l=0}^{U-1}|z_u^{(1)}(l)-\hat{z}(l)|^2+\sum_{l=N}^{2N-1}|z_u^{(1)}(l)-\hat{z}(l)|^2\right)^{1/2}. \tag{2.12}$$

Depending on the ascending sorted $d_u^{(1)}$, $M(M<P^U)$ candidate constellation points are selected to calculate in the next iteration as $\mathbf{Z}_{(k)}^{(1)}$ $(k=1,\ldots,M)$. The $\hat{\mathbf{X}}^{(1)(u)}$ are stored as $\hat{\mathbf{X}}^{(1)(k)}(k=1,\ldots,M)$. Secondly, $\hat{\mathbf{X}}^{(2)(u)}(u=1,\ldots,MP)$=$[\hat{\mathbf{X}}^{(1)(k)}$, $\hat{x}(U)$ $,0,\ldots,0]$ and $\hat{x}(U)\in\{-1,1\}$. Therefore, MP kinds of vector $\mathbf{Z}_u^{(2)}=[z_u^{(2)}(0)$ $\ldots z_u^{(2)}(2N-1)]$ are presented as

$$\mathbf{Z}_u^{(2)}=\mathbf{H_v}\times\hat{\mathbf{X}}^{(2)(u)}. \tag{2.13}$$

(2.14)

The Euclidian distances $d_u^{(2)}(u = 0, \ldots, MP-1)$ between $\mathbf{Z}_u^{(2)}$ and the received samples $\hat{\mathbf{Z}}$ are evaluated by

$$d_u^{(2)} = \left(\sum_{l=0}^{U} |z_u^{(2)}(l) - \hat{z}(l)|^2 + \sum_{l=N}^{2N-1} |z_u^{(2)}(l) - \hat{z}(l)|^2 \right)^{1/2}. \tag{2.15}$$

Thus, $M(M < P^U)$ $\mathbf{Z}_u^{(2)}$ candidate constellation points are selected to calculate in the next iteration as $\mathbf{Z}_{(k)}^{(2)}$ $(k = 1, \ldots, M)$ depending on the Euclidian distances. $\hat{\mathbf{X}}^{(2)(u)}$ are stored as $\hat{\mathbf{X}}^{(2)(k)}(k = 1, \ldots, M)$. Repeat the same operation until $\hat{\mathbf{X}}$ are all evaluated.

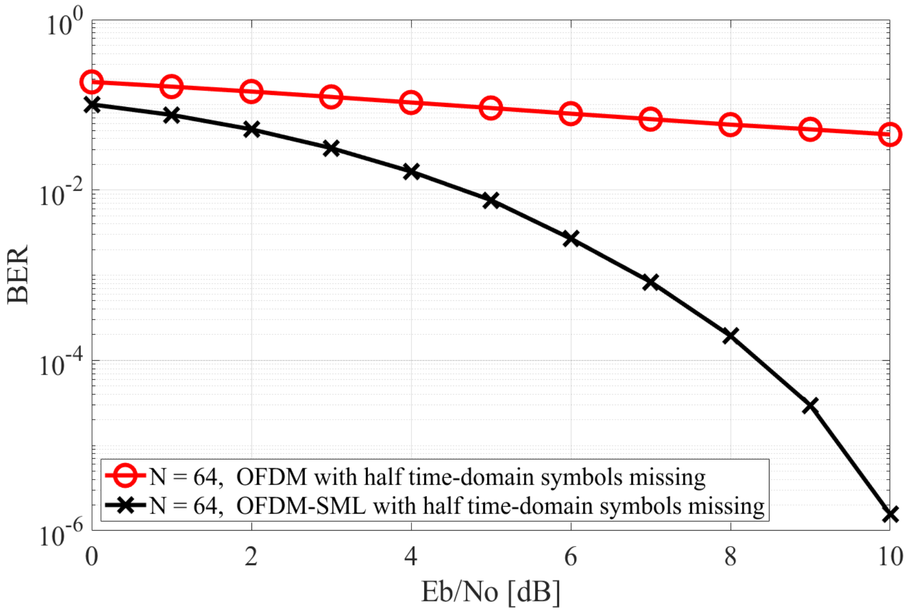

Figure 2.2: BER performance of OFDM-SML compared of that of the conventional OFDM system when half time-domain symbols are missing in the AWGN channel.

2.4 Simulated results

We simulate OFDM-SML over an AWGN channel with the number of the subcarriers $N = 64$ when half time-domain symbols are missing. The BER performance of the proposed system is described in Figure 2.2. Since the SML compares all the possible values with the received signal in every iteration, the BER performance of OFDM-SML is better than that of the conventional OFDM system in the AWGN channel even half time-domain symbols missing.

Table 2.1: Parameters of OFDM-SML

Parameters	Specification
FFT size	64
Guard Interval	1/4
Modulation	BPSK
Equalization	ZF / MMSE
SML (U,M)	(3, 32)
Bandwidth	40MHz
Channel model	WLAN model (Model B)
Propagation scenarios	Indoor

Table 2.2: Model B Power Delay Profile

Tap number	Power [dB]	Delay [ns]
1	0	0
2	-5.43	10
3	-2.52	20
4	5.89	30
5	-9.16	40
6	-12.51	50
7	-15.61	60
8	-18.71	70
9	-21.82	80

We also simulate OFDM-SML in the WLAN channel. Table 2.1 and Table 2.2 [30] are the parameters of OFDM-SML and Model B power delay profile of

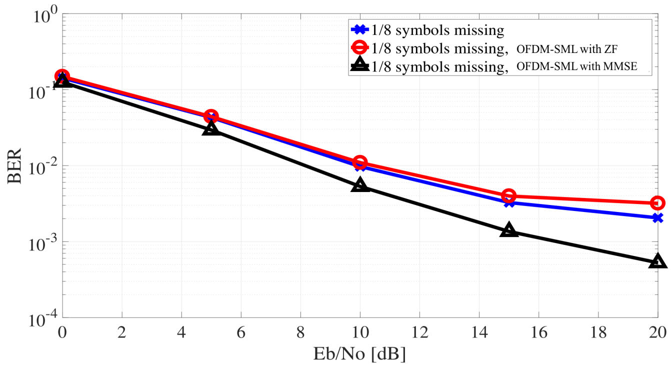

(a) 1/8 time-domain symbols missing

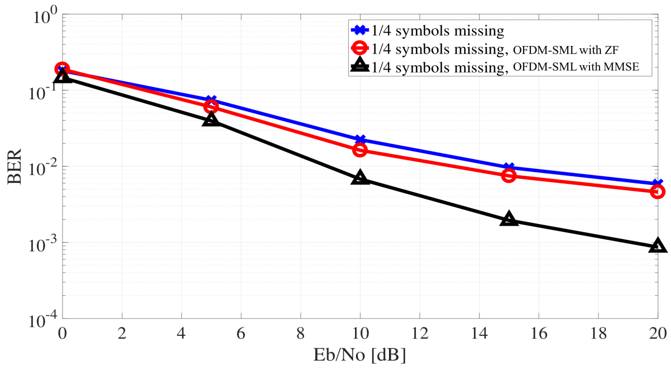

(b) 1/4 time-domain symbols missing

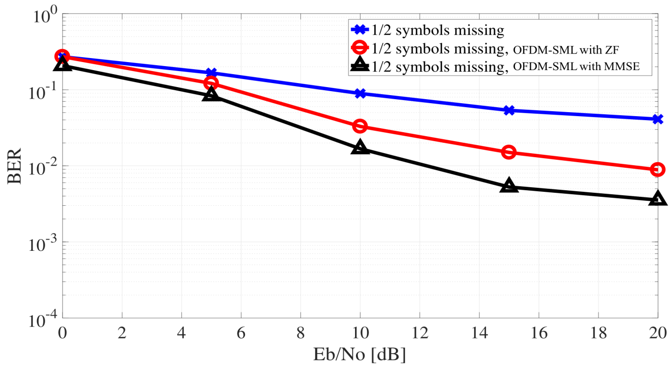

(c) 1/2 time-domain symbols missing

Figure 2.3: BER performance of OFDM-SML with ZF or MMSE and the conventional OFDM system when the time-domain symbols are missing in the WLAN channel model.

the WLAN model, respectively. For SML, we set the number of initial estimators as $U = 3$ and the number of candidate points as $M = 32$. The ZF equalizer simultaneously amplifies the signal and the noise to compensate for the weak signal. However, MMSE equalizer suppresses noise enhancement. Therefore, OFDM-SML using MMSE equalization has better BER performance than that of OFDM-SML using ZF showed in Figure 2.3. However, the BER performance of OFDM-SML using ZF is still better than the conventional OFDM system when 1/4 and 1/2 time-domain symbols are missing.

2.5 Summary

SML is utilized to recover the damaged signal caused by the metallic structure etc. OFDM-SML can obtain better BER performance compared to that of OFDM in the AWGN channel. On the other hand, OFDM-SML with ZF or MMSE can obtain better BER performance than the conventional OFDM in the WLAN channel model. Moreover, the BER performance of the OFDM-SML with MMSE is better than OFDM-SML with ZF.

3 OFDM-SMLB

3.1 Introduction

The damaged signal is not only caused by obstacles such as metallic structures but also caused by IN. Next, we discuss two popular IN models.

3.2 Impulsive noise model

Many IN models have been proposed in the decades. Here we mainly introduce two famous IN models: Bernoulli-Gaussian noise model and Middleton Class A noise model.

3.2.1 Bernoulli-Gaussian noise model

Bernoulli-Gaussian noise model (BG) is widely utilized to analyze the IN in the literature [31, 32]. It is composed of background noise $w(k)$ and impulsive noise $i(k)$, and it is given by

$$n(k) = w(k) + i(k). \tag{3.1}$$

Here the impulsive noise $i(k)$ term is expressed as

$$i(k) = b(k) * g(k), \tag{3.2}$$

where $g(k)$ is the complex white Gaussian noise with zero mean and $\alpha\sigma_g^2$ variance (i.e. α shows that how larger the impulsive noise is than the background noise). $b(k)$ is the Bernoulli process with probability $G(b(k) = 1) = q$ (i.e. $G(b(k) = 0) = 1 - q$). The Probability Density Function (PDF) of the BG shown in Figure

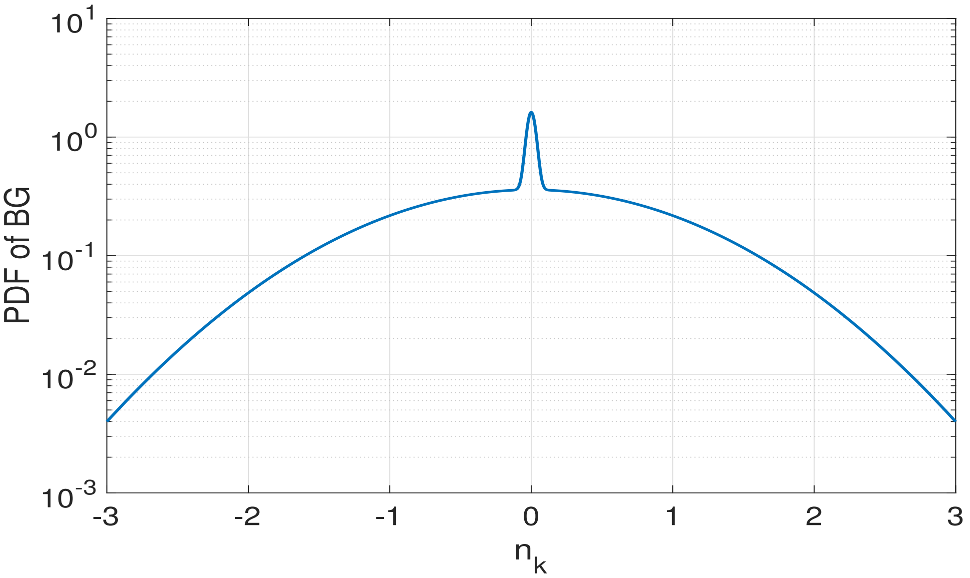

Figure 3.1: PDF of BG with $\sigma_g^2 = 0.001$, $q = 0.1$ and $\alpha = 1000$.

3.1 is described as

$$F(n(k)) = (1-q)\mathcal{N}(n(k); 0, \sigma_g^2) + q\mathcal{N}(n(k); 0, \alpha\sigma_g^2), \tag{3.3}$$

where q is the probability of the IN occurrence and $\mathcal{N}(n(k), 0, \sigma_m^2)$ follows the Gaussian distribution.

3.2.2 Middleton Class A noise model

Middleton developed three kinds of models which are Class A, Class B and Class C [33]. The bandwidth of noise in Middleton Class A (MCA) is narrower than that of the receiver. The noise in Middleton Class B has a larger bandwidth than that of the receiver. Middleton Class C is the sum of Middleton Class A and Middleton Class B. Among them, MCA is a popular IN model in communication systems [32, 34]. The PDF of MCA shown in Figure 3.2 is expressed as

$$F(n(k)) = \sum_{m=0}^{\infty} P_m \mathcal{N}(n(k); 0, \sigma_m^2), \tag{3.4}$$

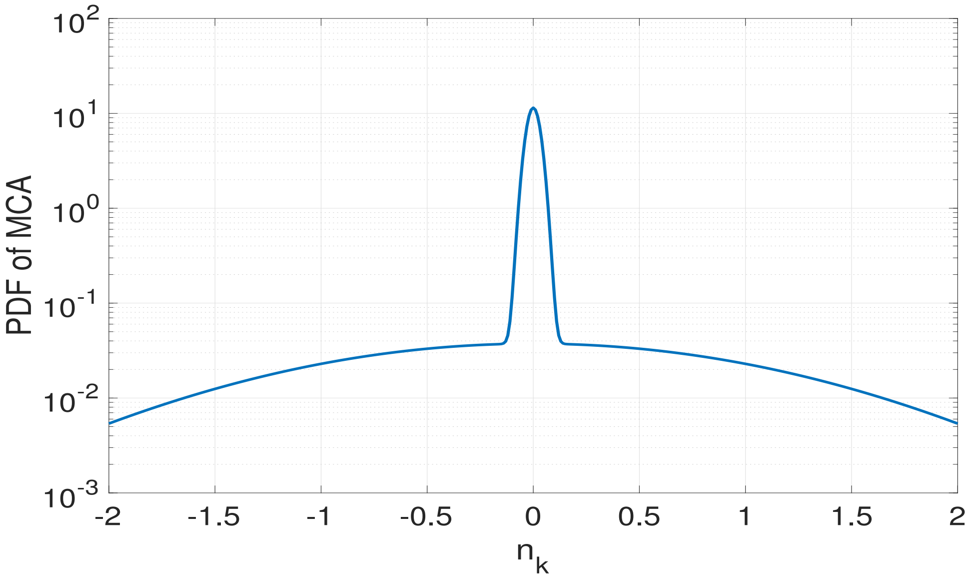

Figure 3.2: PDF of MCA with $\sigma_g^2 = 0.001$, $A = 0.1$ and $\Gamma = 0.01$.

with

$$P_m = \frac{A^m e^{-A}}{m!}. \tag{3.5}$$

$\mathcal{N}(n(k), 0, \sigma_m^2)$ follows the Gaussian distribution with mean 0 and variance σ_m^2 given by

$$\sigma_m^2 = \sigma_g^2 \left(\frac{m}{A\Gamma} + 1 \right), \tag{3.6}$$

where A is the density of the IN in the observation period and $\Gamma = \frac{\sigma_g^2}{\sigma_i^2}$. Here σ_g^2 is the variance of the background noise and σ_i^2 is the variance of IN term.

3.3 Conventional methods

Researchers have proposed many methods to mitigate the impact of the IN. Here we describe two methods including blanking or clipping at the receiver and interleaving at the transmitter.

3.3.1 Blanking and Clipping

Blanking and clipping are conventional methods to reduce the impact of the IN [35] - [39]. Mathematical equations are shown in the following expressions.

(1) Blanking

$$\hat{\mathbf{y}}_p = \begin{cases} \mathbf{y}_p & |\mathbf{y}_p| \leqslant T_B \\ 0 & otherwise \end{cases}, \tag{3.7}$$

where $\mathbf{y}_p$ is the received signal and T_B is the blanking threshold. As equation shown, when the signal is above the threshold, it is regarded as the IN and then set its value to zero.

(2) Clipping

$$\hat{\mathbf{y}}_p = \begin{cases} \mathbf{y}_p & |\mathbf{y}_p| \leqslant T_C \\ T_C e^{j\arg(\mathbf{y}_p)} & otherwise \end{cases}, \tag{3.8}$$

where T_C is the clipping threshold. Note that the phase of these methods is not modified. Different from blanking scheme, the value of the detected IN is related to the threshold. Therefore, these two methods are sensitive to the threshold and it is important to select the proper threshold.

3.3.2 Interleaving

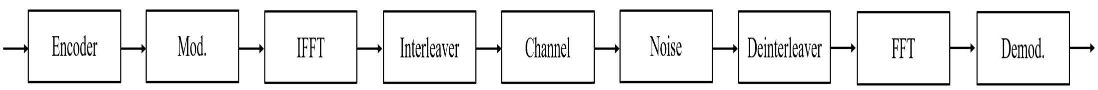

Figure 3.3: Structure of the system with interleaving.

Besides the methods mentioned above, interleaving is implemented in the transmitter to improve the performance of the system [40] shown in Figure 3.3. Ref. [41] proposed to implement interleaving after IFFT. Unlike the conventional

OFDM system which utilizes interleaving before IFFT, the aim is to spread the contaminated samples over a large number of OFDM symbols and then improve the performance at a little cost of complexity.

3.4 Proposed system

OFDM can cope well with the IN when the noise power is moderate. However, IN results in more errors even OFDM system in the high probability of IN occurrence (high q) and high IN power (i.e., it is proportional to α). The combination of OFDM and blanking or clipping are the conventional methods to reduce the impact of the IN. The drawback of these methods is degrading the performance when the useful signal is mistaken as the IN. Therefore, it is challenging to obtain the optimal threshold to judge the true useful signal or the IN. Reference [35] has proposed a method to find the theoretical threshold value, and Ref. [38] further proposed an adaptive threshold maximizing the signal-to-interference-and-noise ratio (SINR) to mitigate the impact of the IN. However, these methods require the parameters of the impulsive noise model and only take account of the non-fading channel. On the other hand, Ref. [42] has proposed the MLSE decoding to improve the performance of single carrier systems over the environments with large IN. Although the system delivers good performance, the complexity is very high. Significantly, the complexity of OFDM with MLSE increases exponentially with the number of subcarriers.

We propose OFDM-SMLB which combines Suboptimal MLSE and Blanking (SMLB) to improve the performance with an acceptable complexity. Furthermore, OFDM-SMLB utilizes Constant False Alarm Rate (CFAR) [43] to obtain the location of the IN by distinguishing the mixed signal, including transmitted signal, background noise, and the IN term [44,45]. The OFDM-SMLB is discussed in detail in the following section.

3.4.1 System model

Let $\mathbf{X}_p = [x_p(0), \ldots, x_p(N-1)]^T$ represent the M-QAM modulated data stream in the frequency-domain with N subcarriers in the pth OFDM symbol. Figure 3.4 shows that the modulated data bits are transmitted through IFFT and CP to

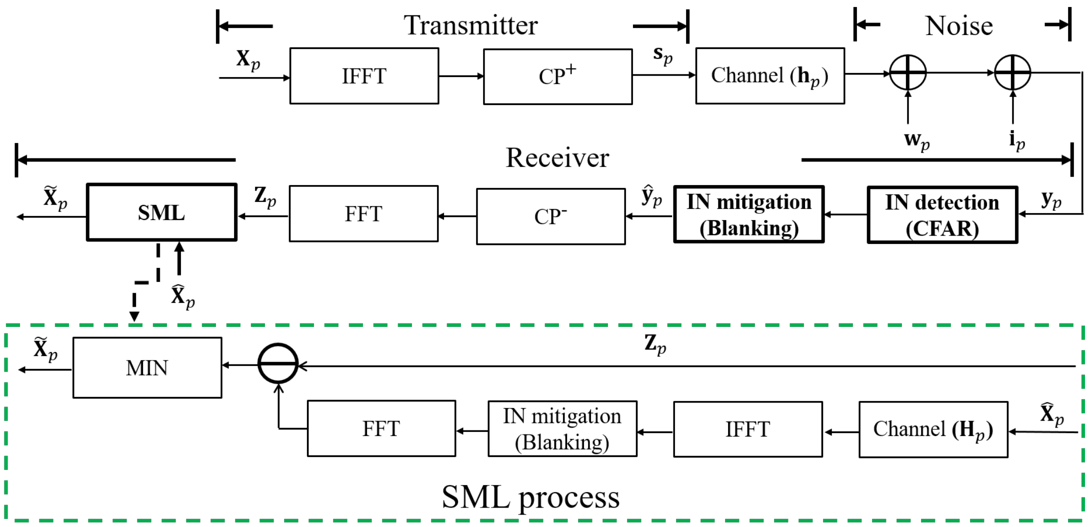

Figure 3.4: Structure of the OFDM-SMLB.

obtain the time-domain symbols $\mathbf{s}_p = [s_p(N-N_{cp}), ..., s_p(N-1), s_p(0), \ldots, s_p(N-1)]^T$. Here N_{cp} is the length of CP and the power of the transmitted signal σ_s^2 is calculated as $\frac{1}{2}E\{|\mathbf{s}_p|^2\}$.

In this paper, BG is utilized as the IN model for the convenience of analyzing the performance of the proposed system. Note that it can be extended to the other famous IN models such as MCA. The noise is given by

$$\mathbf{n}_p = \mathbf{w}_p + \mathbf{i}_p \tag{3.9}$$

where $\mathbf{w}_p = [w_p(0), \ldots, w_p(N-1)]^T$ is the background noise and $\mathbf{i}_p = [i_p(0), \ldots, i_p(N-1)]^T$ is the IN.

At the receiver side, the received symbols $\mathbf{y_p}$ are expressed as

$$\mathbf{y}_p = \mathbf{h}_p \otimes \mathbf{s}_p + \mathbf{w}_p + \mathbf{i}_p \tag{3.10}$$

where $\mathbf{h}_p = [h_p(0), h_p(1), 0, \ldots, 0]^T$ is the channel impulse response for the two-path Rayleigh fading model. Thus, the part whose power is greater than the threshold is blanked in the received symbols. Here, the threshold can be derived based on the variance of the received symbols σ_r^2 and the probability of false-alarm (P_{fa}). The system assumes that the OFDM signal can be modeled as a complex Gaussian process with Rayleigh envelope distribution when the number of subcarriers is sufficiently large [37] in the case of the only AWGN exists. Based on [37], the received symbols $|\mathbf{y}_p|$ follow the Rayleigh distribution. The P_{fa} of $|\mathbf{y}_p|$ is expressed as

$$F_{Pfa}(T_B;\sigma_r^2) = e^{(-\frac{T_B^2}{2\sigma_r^2})}, \tag{3.11}$$

where T_B is the blanking threshold. Therefore, T_B can be obtained as

$$T_B = \sqrt{-2\sigma_r^2 \ln(F_{Pfa})}, \tag{3.12}$$

given F_{Pfa}. The blanked symbols are described as

$$\hat{\mathbf{y}}_p = \begin{cases} \mathbf{y}_p & |\mathbf{y}_p| \leqslant T_B \\ 0 & otherwise \end{cases}. \tag{3.13}$$

After removing CP and accomplishing FFT, we utilize SML to reconstruct the original symbols. The output of SML can be represented as

$$\tilde{\mathbf{X}}_p = \arg\min |\mathbf{Z}_p - \mathbf{H}_p\hat{\mathbf{X}}_p|^2 \tag{3.14}$$

with $\mathbf{Z}_p = [z(0),\ldots,z(N-1)]^T$, $\hat{\mathbf{X}}_p = [\hat{x}(0),\ldots,\hat{x}(N-1)]^T$ and $\hat{x}(i) \in \{-1,1\}$ for BPSK. Here we assume that the channel is perfectly detected. Therefore, $\mathbf{H}_p$ can be written as

$$\mathbf{H}_p = \begin{bmatrix} H_p(0) & 0 & \ldots & 0 \\ 0 & H_p(1) & \ldots & 0 \\ \vdots & \vdots & \ldots & \vdots \\ 0 & 0 & \ldots & H_p(N-1) \end{bmatrix}. \tag{3.15}$$

As we know, the computational complexity of MLSE used in the OFDM system increases exponentially as N^P with the number of subcarriers N and the number of constellation subsets P (i.e., $P \in \{-1,1\}$ for BPSK). In order to reduce the complexity, the proposed system utilizes SML whose complexity increases linearly as MP by limiting the candidate constellation points to a given number M in every iteration.

We define $\hat{\mathbf{X}}^{(i)(j)}$ as the jth candidate constellation points of the ith iteration process. Note that we omit the subscript p of the above-mentioned parameters for the convenience of analyzing the impact of SML. The steps of SML can be described as follows:

Step 1: Assume that P is the number of constellation subset of $\{-1, 1\}$ for BPSK. We define N points as $\hat{\mathbf{X}}^{(1)(u)}$ =$[\hat{x}(0), \ldots, \hat{x}(U-1), \ldots, 0]$ with $\hat{x}(k) \in \{-1, 1\}$ and $k \in [0, \ldots, U-1]$. In other words, there are P^U kinds of $\hat{\mathbf{X}}^{(1)(u)}$ (i.e. $u \in [1, \ldots, P^U]$). Note that U denotes the number of candidate constellation points in the first iteration process. $\hat{\mathbf{Z}}_u^{(1)} = [z_u^{(1)}(0), \ldots, z_u^{(1)}(N-1)]$ are presented as

$$\hat{\mathbf{Z}}_u^{(1)} = \mathbf{H}\hat{\mathbf{X}}^{(1)(u)}. \tag{3.16}$$

Therefore, the Euclidian distances $d_u^{(1)}$ between $\hat{\mathbf{Z}}_u^{(1)}$ and received samples $\mathbf{Z}$ are evaluated as

$$d_u^{(1)} = \sum_{l=0}^{U-1} |\hat{z}_u^{(1)}(l) - z(l)|. \tag{3.17}$$

Here there are P^U kinds of $\hat{\mathbf{Z}}_u^{(1)}$ generated. After sorting $d_u^{(1)}$ by ascending order, the corresponding first $M(M < P^U)$ $\hat{\mathbf{Z}}_u^{(1)}$ are selected to continue to the next iteration as $\hat{\mathbf{Z}}_{(r)}^{(1)}$ $(r = 1, \ldots, M)$ with corresponding $\hat{\mathbf{X}}^{(1)(u)}$ which are stored as $\hat{\mathbf{X}}^{(1)(r)}$ $(r = 1, \ldots, M)$.

Step 2: Redefine the N samples $\hat{\mathbf{X}}^{(2)(u)}$ $(u = 1, \ldots, MP)$ as $\hat{\mathbf{X}}^{(2)(u)}$=$[\hat{\mathbf{X}}^{(1)(r)}, \hat{x}(i), 0, \ldots, 0]$ and $\hat{x}(i) \in \{-1, 1\}$. Therefore, MP kinds of vector $\hat{\mathbf{Z}}_u^{(2)} = [\hat{z}_u^{(2)}(0), \ldots \hat{z}_u^{(2)}(N-1)]$ are presented as

$$\hat{\mathbf{Z}}_u^{(2)} = \mathbf{H}\hat{\mathbf{X}}^{(2)(u)}. \tag{3.18}$$

The Euclidian distances $d_u^{(2)}(u = 0, \ldots, MP-1)$ between $\hat{\mathbf{Z}}_u^{(2)}$ and the received samples $\mathbf{Z}$ are evaluated by

$$d_u^{(2)} = \sum_{l=0}^{U} |\hat{z}_u^{(2)}(l) - z(l)|. \tag{3.19}$$

The first M $\hat{\mathbf{Z}}_u^{(2)}$, which are smaller Euclidian distances, are selected as $\hat{\mathbf{Z}}_{(r)}^{(2)}(r = 1, \ldots, M)$ from MP kinds of $\hat{\mathbf{Z}}_u^{(2)}$ with corresponding $\hat{\mathbf{X}}^{(2)(u)}$ which are stored as $\hat{\mathbf{X}}^{(2)(r)}$=$[\hat{x}(0), \ldots, \hat{x}(U-1), \hat{x}(U)](r = 1, \ldots, M)$.

Step 3: MP kinds of $\hat{\mathbf{Z}}_u^{(N-U+1)}$ are obtained by repeating Step 2 $(N-U)$ times. Finally, the vector $\hat{\mathbf{X}}^{(N-U+1)(1)}$, which is the minimum Euclidian distance, is the desired result.

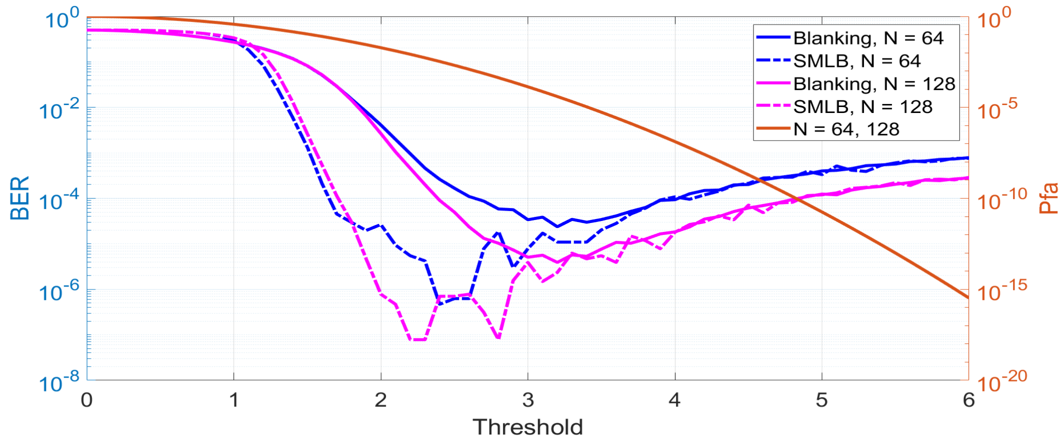

(a) $q = 0.01, \alpha = 1000$

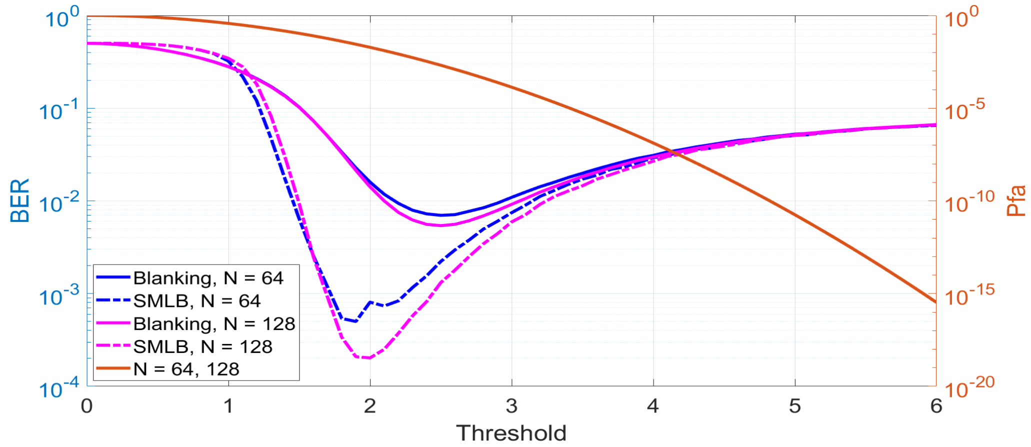

(b) $q = 0.1, \alpha = 1000$

Figure 3.5: P_{fa} vs Threshold, BER performance vs Threshold for comparison of the conventional blanking system and OFDM-SMLB without CFAR detector in the non-multipath fading channel with $q = 0.01, 0.1$ and $\alpha = 1000$ given Eb/No = 20dB when $N = 64, 128$.

3.4.2 Performance evaluation

(1) Proposed receiver for the non-multipath fading channel

The P_{fa} versus Threshold and BER performance versus Threshold are described in Figure 3.5. The proposed system can obtain better performance than that of the conventional blanking system in a certain range. For example, Figure 3.5(a) shows that the best BER of the conventional blanking system is 9.4×10^{-5}, whereas the best BER of OFDM-SMLB is 7.8×10^{-8} (i.e., $N = 128$). Thus in Figure 3.5(b), the BER of the proposal can reach 2.0×10^{-4} (i.e., $N = 128$) compared to that of the conventional blanking system whose BER is 5.4×10^{-3} in the optimal threshold. The numerous simulated results show that it is the optimal threshold when P_{fa} is about 1.0×10^{-3} (i.e., $q = 0.01$) and P_{fa} is about 1.0×10^{-2} (i.e., $q = 0.1$) given Eb/No = 20dB. Implicitly, OFDM-SMLB has the best BER value with $P_{fa} = 1.0 \times 10^{-3}$ in Figure 3.5(a) and $P_{fa} = 1.0 \times 10^{-2}$ in Figure 3.5(b) when Eb/No = 20dB. Moreover, the BER performance with $N = 128$ is better than that of $N = 64$ in both systems.

Figure 3.6 shows the performance of the conventional blanking or clipping OFDM system and OFDM-SMLB. The OFDM-SMLB can obtain good performance compared to that of the conventional with or without blanking or clipping process. For example, in Figure 3.6(a), OFDM-SMLB can obtain about 10dB Eb/No improvement to achieve BER = as 1.9×10^{-5} when $P_{fa} = 0.001$. On the other hand, the curve in Figure 3.6(b) is increasing upward after Eb/No = 15dB, but it is still better than that of the conventional system. The reason is that when Eb/No becomes larger, the power of the Gaussian noise becomes smaller. However, the IN and the expected signal are mixed due to large α, although the expected signal can be separated from the background noise. Besides, the performance of the OFDM with blanking may be better than that of OFDM with clipping (e.g., Figure 3.6(b)) which has a similar conclusion as Reference [35]. Note that SML itself does not have an impact on the performance in the IN environment. As a matter of fact, Ref. [46, 47] has mentioned that the SML can recover a partial duration of the OFDM symbols (i.e., add zeros at the end of the received partial signal) under the assumption of only AWGN noise existence. Namely, the combination of SML and zero addition used to replace the missing

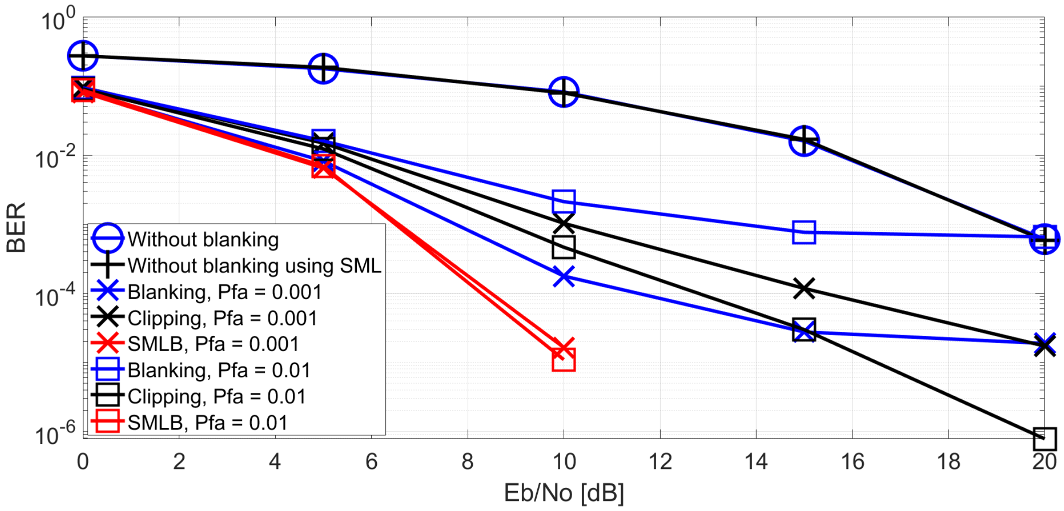

(a) $q = 0.01, \alpha = 1000$

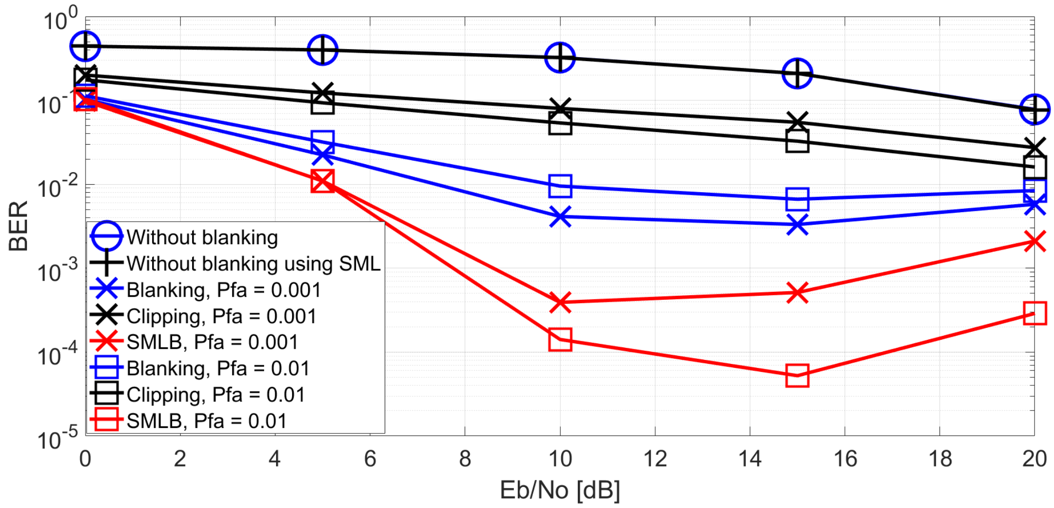

(b) $q = 0.1, \alpha = 1000$

Figure 3.6: BER performance vs Eb/No for comparison of the conventional with or without blanking system and OFDM-SMLB in the non-multipath fading channel with $q = 0.01, 0.1$ and $\alpha = 1000$ given P_{fa} ($P_{fa} = 0.001$ and 0.01).

part can improve the performance in the AWGN noise. In our case, the blanked part, which is regarded as the IN, is set to zero (i.e., the other part is only affected by AWGN), SML recovers the blanked signal.

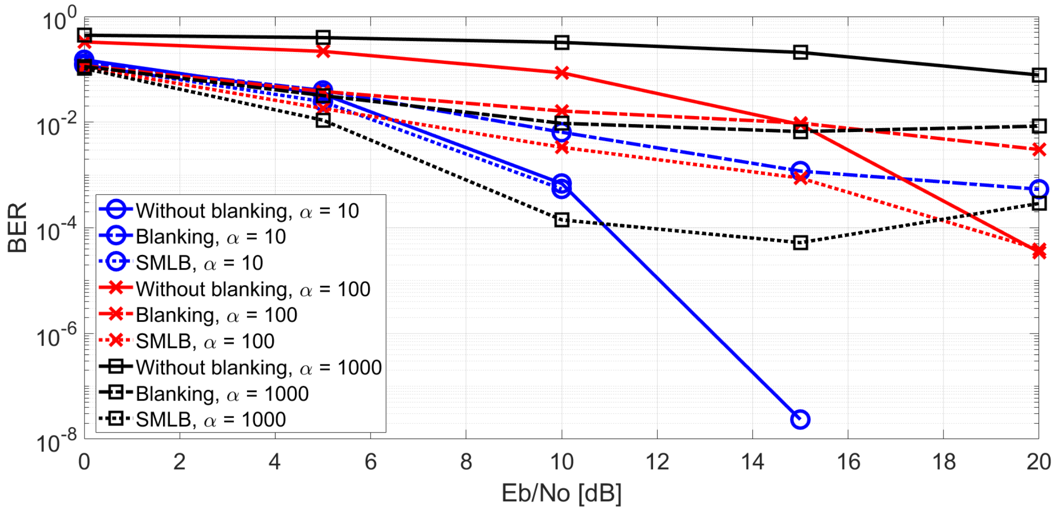

Figure 3.7: BER performance vs Eb/No for comparison of the conventional with or without blanking system and OFDM-SMLB in the non-multipath fading channel with $q = 0.1$ and $\alpha = 10, 100, 1000$ given $P_{fa} = 0.01$.

Figure 3.7 shows the BER performance of OFDM-SMLB versus conventional with and without blanking system when $q = 0.1$ and different α. The simulated results show that OFDM-SMLB can improve the performance with increasing α compared to that of the conventional system. When α is small, it is difficult to distinguish the difference between the symbols affected by only background noise or impulsive noise. In other words, the blanked signal has a high probability of being wrongly regarded as the IN, and it turns out to degrade the performance of the system. However, when α is large, OFDM-SMLB can further improve the BER performance of the OFDM with blanking system. Moreover, generally, moderate or high q and α are more valuable to discuss since IN is a dominant factor affecting the performance of the system.

On the other hand, OFDM-SMLB can adjust the number of candidates (i.e. $M = 32$ in this paper) to meet the demand of the trade-off between the BER performance and complexity. The complexity of the OFDM-SMLB is $P^{U+k} \times (N-$

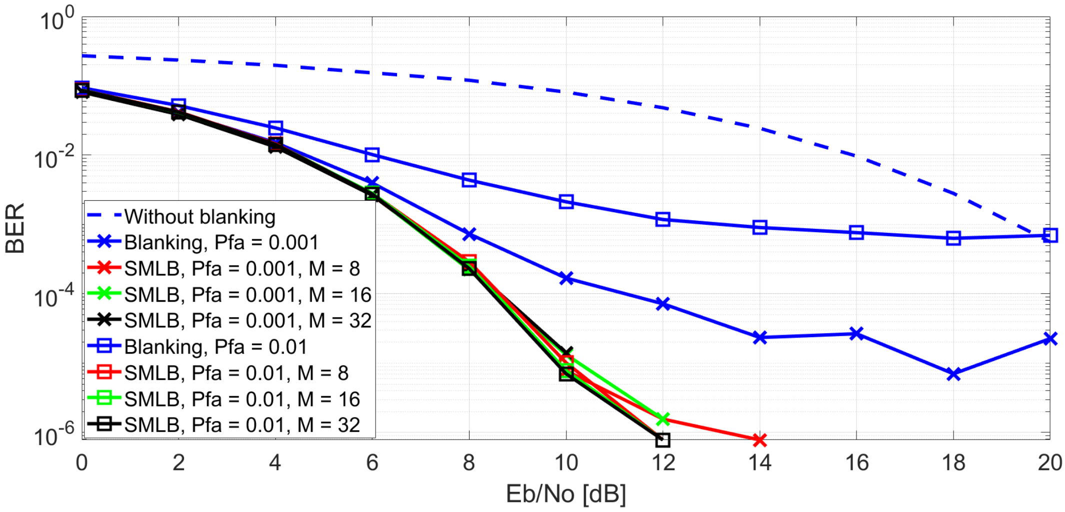

(a) $q = 0.01, \alpha = 1000$

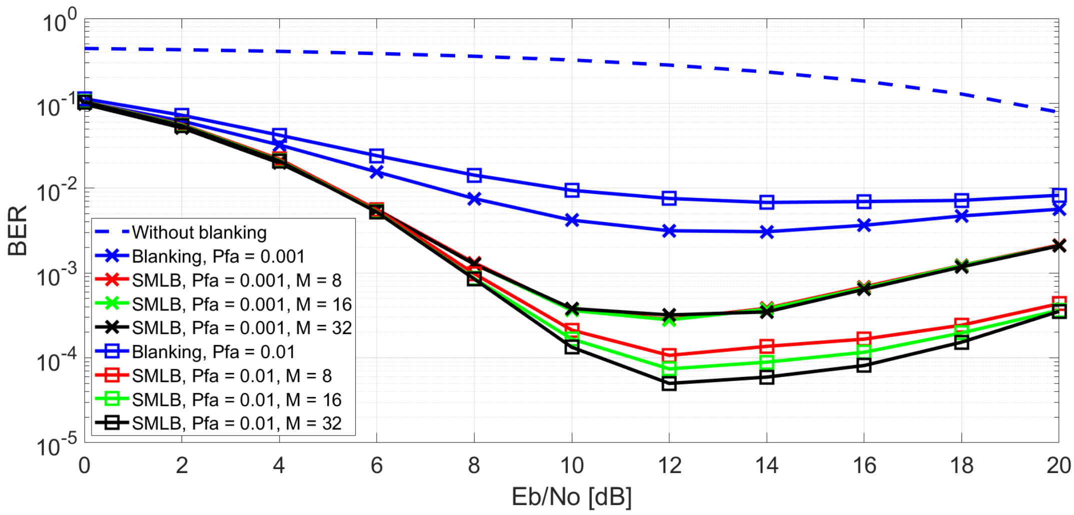

(b) $q = 0.1, \alpha = 1000$

Figure 3.8: BER performance vs Eb/No for comparison of the conventional with or without blanking system and OFDM-SMLB using different number of candidates (M) in the non-multipath fading channel with $q = 0.01, 0.1$ and $\alpha = 1000$ given P_{fa} ($P_{fa} = 0.001$ and 0.01) when $N = 128$.

$U - k)(MP)$. Note that M is the number of the candidates in every iteration, P

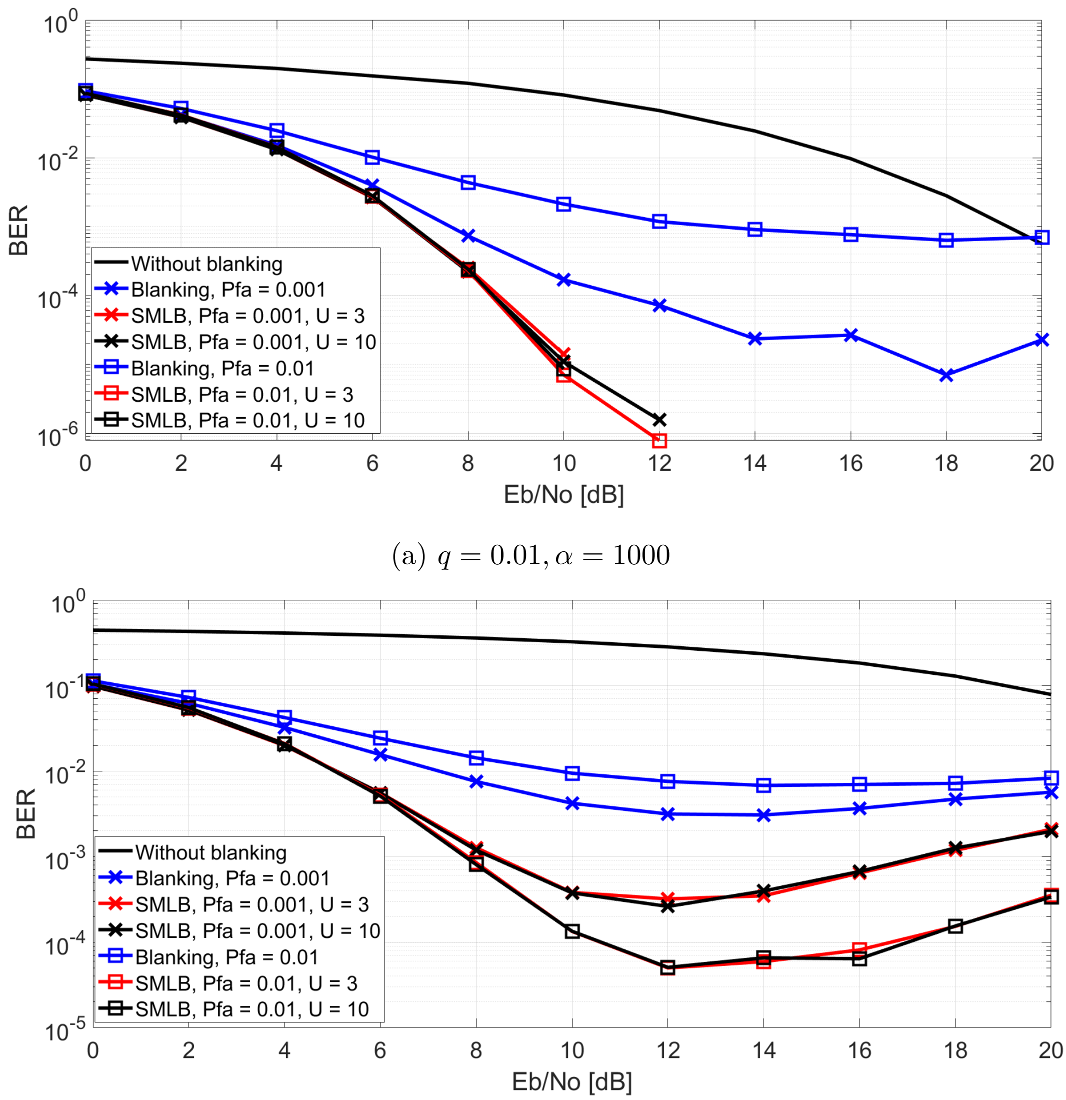

(a) $q = 0.01, \alpha = 1000$

(b) $q = 0.1, \alpha = 1000$

Figure 3.9: BER performance vs Eb/No for comparison of the conventional with or without blanking system and OFDM-SMLB using different initial number of subcarriers (U) in the non-multipath fading channel with $q = 0.01, 0.1$ and $\alpha = 1000$ given P_{fa} ($P_{fa} = 0.001$ and 0.01) when $N = 128$.

is the number of the constellation, U is the initial number of subcarriers utilized,

N is the number of the subcarriers and k is the $(k+1)$th iteration where the number of candidates is less than M. In this paper, the complexity of OFDM-SMLB is $2^5 \times (123 \times 32 \times 2)$ with $M = 32, P = 2, N = 128$ and $U = 3$. When $M = 16$, the complexity is $2^4 \times (124 \times 16 \times 2)$ etc. Figure 3.8(a) shows that when $q = 0.01, \alpha = 1000$, the BER performance of the system with $M = 8, 16$ is almost the same as that of the system with $M = 32$. When $q = 0.1$ described in Figure 3.8(b), OFDM-SMLB has worse degradation with M decreasing (i.e., P_{fa} = 0.01). However, it still has better performance than that of the conventional blanking scheme.

Besides M, U is another parameter of SML method. When $U <= \log_2 M$, the performance or complexity of the system is the same as that of the system with $U = \log_2 M$, since the removed possible candidates start from the case that the number of candidates is larger than M. When $U > \log_2 M$, the complexity is increasing with larger U. The BER performance versus Eb/No with different U is described in Figure 3.9. The simulated results show that small or moderate U has no effect on the performance of the system whether moderate or high q and α. For high U, the complexity of the system is approaching that of the system using MLSE. Therefore, it is not meaningful from the view of SML concept.

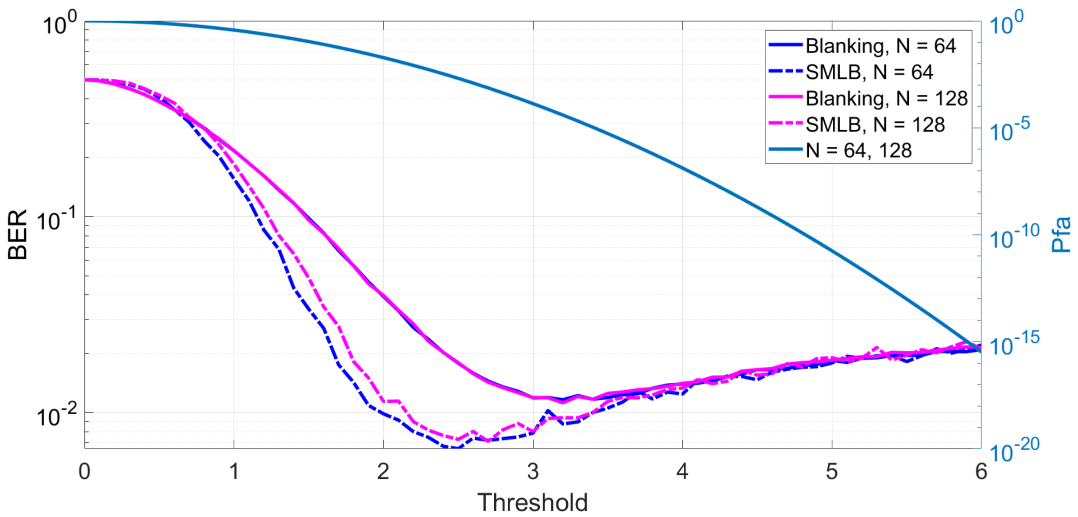

(a) $q = 0.01, \alpha = 1000$

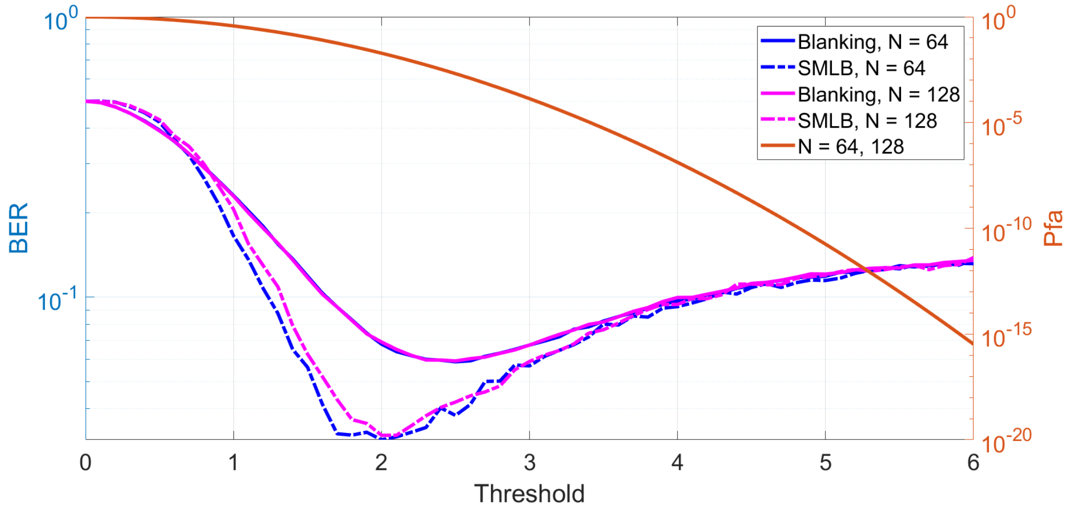

(b) $q = 0.1, \alpha = 1000$

Figure 3.10: P_{fa} vs Threshold, BER performance vs Threshold for comparison of the conventional blanking system and OFDM-SMLB without CFAR detector in the two-path Rayleigh fading channel with $q = 0.01, 0.1$ and $\alpha = 1000$ given Eb/No = 20dB when $N = 64, 128$.

(2) Proposed receiver for the multipath fading channel

Figure 3.10 describes the P_{fa} versus Threshold and BER performance versus Threshold in the two-path Rayleigh fading channel. The simulated results show that OFDM-SMLB can further improve the BER performance of OFDM with blanking when the appropriate threshold is chosen.

Table 3.1: Parameter and configuration of OFDM-SMLB.

Parameter	Configuration
FFT size	128
Number of Symbols	10
CP	32
Modulation	BPSK
q	0.01, 0.1
α	10, 1000
Channel Model	Two-path Rayleigh fading channel
Noise Model	Bernoulli-Gaussian noise model
Channel Estimation	Perfect Channel Estimation
SML (U, M)	(3, 32)

(U, M): U is the number of subcarriers used in the first iteration and M is the number of the candidate values in every iteration.

The parameter and configuration of the proposed system in the two-path Rayleigh fading channel are shown in Table 3.1. Figure 3.11 shows that when $\alpha = 1000$, OFDM-SMLB has better performance than the conventional with or without blanking and clipping system. For example, OFDM-SMLB can achieve about 7dB Eb/No improvement with BER $= 2 \times 10^{-2}$ given $P_{fa} = 0.001$ in Figure 3.11(a). Therefore, OFDM-SMLB can achieve performance improvement by adjusting P_{fa} value when α is very large.

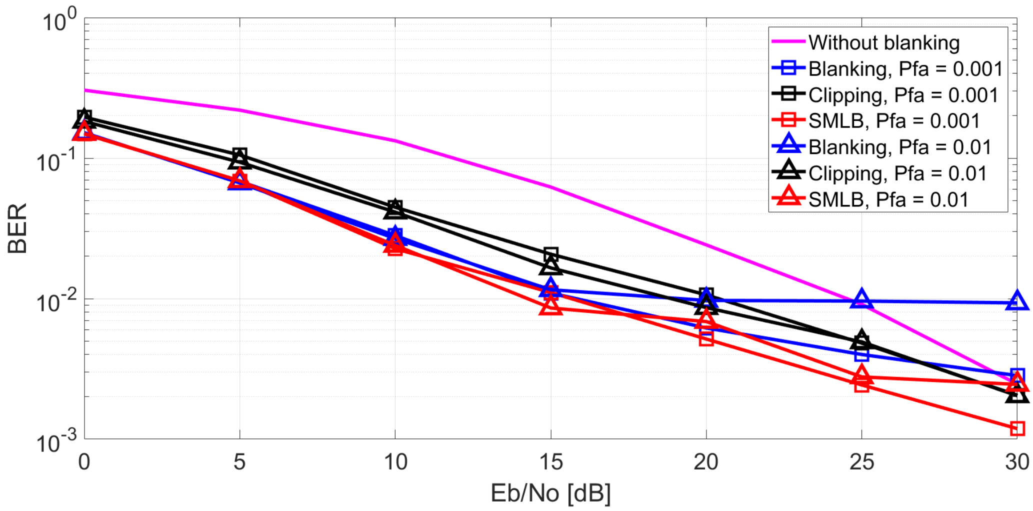

(a) $q = 0.01, \alpha = 1000$

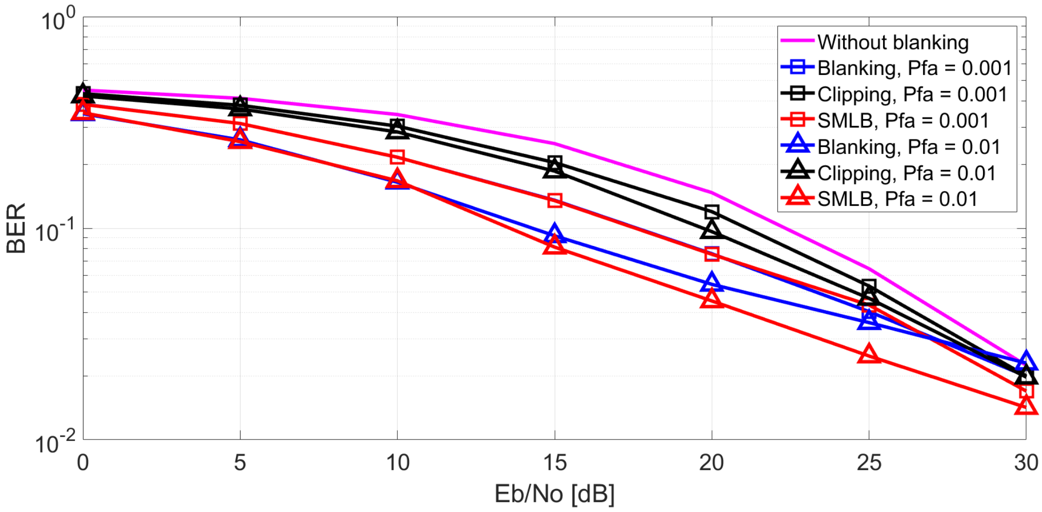

(b) $q = 0.1, \alpha = 1000$

Figure 3.11: BER performance vs Eb/No for comparison of the conventional with or without blanking system and OFDM-SMLB in the two-path Rayleigh fading channel with $q = 0.01, 0.1$ and $\alpha = 10, 1000$ given P_{fa} ($P_{fa} = 0.001$ and 0.01).

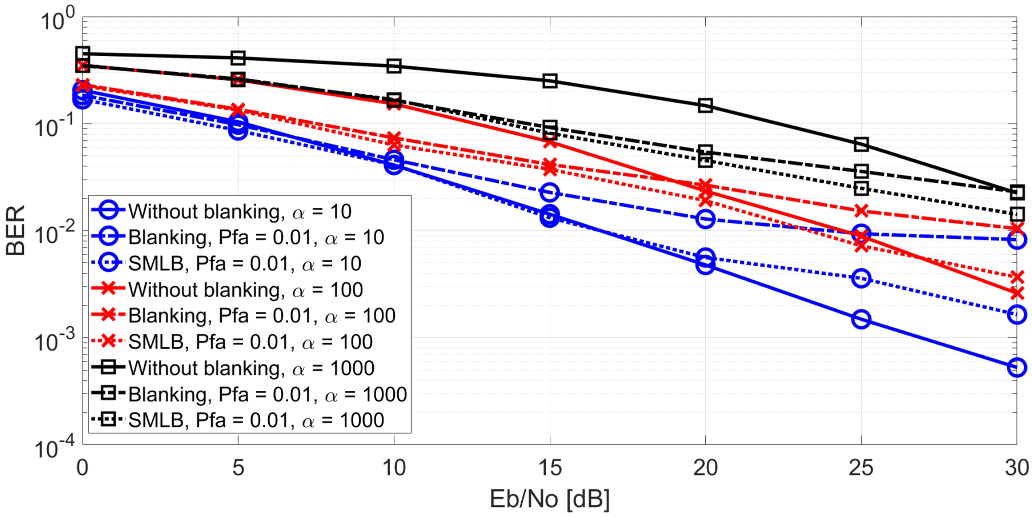

Figure 3.12: BER performance vs EbNo for comparison of the conventional with or without blanking system and OFDM-SMLB in the two-path Rayleigh fading channel with $q = 0.1$ and $\alpha = 10, 100, 1000$ given P_{fa} ($P_{fa} = 0.01$).

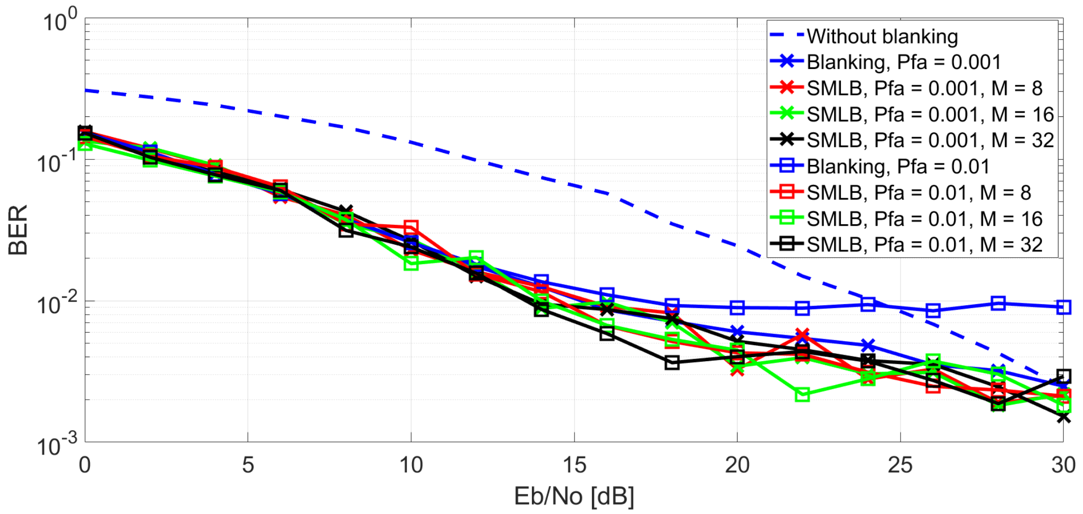

(a) $q = 0.01, \alpha = 1000$

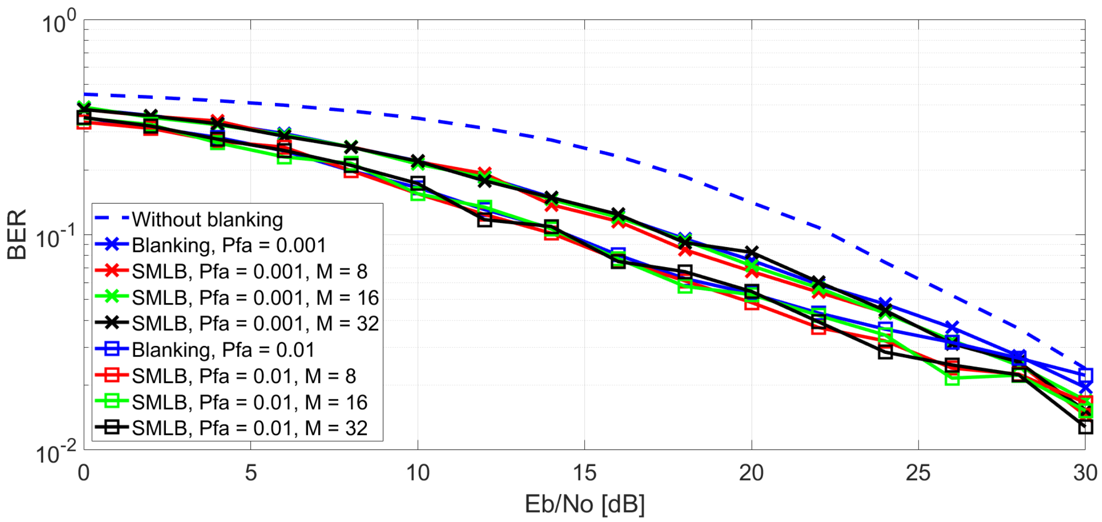

(b) $q = 0.1, \alpha = 1000$

Figure 3.13: BER performance vs Eb/No for comparison of the conventional with or without blanking system and OFDM-SMLB using different number of candidates (M) in the two-path Rayleigh fading channel with $q = 0.01, 0.1$ and $\alpha = 1000$ given P_{fa} ($P_{fa} = 0.001$ and 0.01) when $N = 128$.

Figure 3.12 describes the performance of the OFDM-SMLB with α varying in the fading channel. When $\alpha = 10$, the blanking method is not useful, whereas the SMLB method can improve the performance of the blanking. When $\alpha = 100$, the performance is close to that of the system without blanking. The proposed system can achieve about 5dB Eb/No improvement with BER $= 2 \times 10^{-2}$ given $P_{fa} = 0.01$ when $\alpha = 1000$. Therefore, OFDM-SMLB can obtain better performance than the system with or without blanking.

In Figure 3.13, the performance of OFDM-SMLB with $M = 8$ is almost the same as that of the system with $M = 32$ whether $q = 0.01$ or $q = 0.1$. Therefore, the complexity can be further reduced compared to that of the system with $M = 32$ in the Rayleigh fading channel.

3.5 Summary

we proposed SMLB based OFDM receiver to mitigate the impact of the IN. The simulated results showed that the proposed system can further improve the performance of OFDM with blanking for high frequent IN occurrence (high q) and high IN power (large α) with an appropriate threshold. We pointed out that the proposed system can achieve the trade-off between the performance and the complexity by adjusting the M value. It was useful to mitigate the degradation of the system in the harsh industrial factory at the acceptable cost of complexity.

4 Conclusions and future research

4.1 Conclusions

In this thesis, we solve two situations in the harsh industry: 1) Damaged signal caused by metallic pillars and machines and 2) Impulsive noise. OFDM-SML is utilized to recover the damaged signal. In addition, OFDM-SMLB can mitigate the impact of IN with an acceptable and flexible complexity.

Chapter 1 described the current situation of the smart factory in the industry and introduced the important technique – OFDM. In some scenarios such as manufacturing and automatic factories, the OFDM system suffered from the damaged time-domain signal due to metallic pillars and impulsive noise.

In Chapter 2, we described the OFDM-SML in detail. After the introduction of the structure of the OFDM-SML, we analyzed the performance of the proposed system. OFDM-SML can obtain better BER performance compared to that of OFDM in the AWGN channel. On the other hand, OFDM-SML with ZF or MMSE can obtain better BER performance than OFDM in the WLAN channel model. Moreover, the BER performance of OFDM-SML with MMSE is better than that of the conventional OFDM-SML with ZF.

In Chapter 3, we explained OFDM-SMLB using CFAR. CFAR is utilized to detect the location of the IN and then blank these IN. The SMLB can reconstruct the original frequency-domain signal. The simulated results showed that the proposed system can obtain better BER performance than the conventional with or without blanking system with an acceptable complexity for the non-multipath fading and multipath fading channel. Furthermore, the proposed system can further improve the performance of the conventional blanking system for high frequent IN occurrence (high q) and high IN power (large α).

4.2 Future research

As mentioned above, the blanking method is not applicable for small α for both conventional and proposed systems. Therefore, it is vital to estimate the α to decide whether the proposed system should be utilized. However, it is difficult to directly estimate the α since it is related to the characteristics of the noise model. The indirect method is to increase the accuracy of the detection of IN location to improve the performance. Ref. [48] has proposed the two stages which are to utilize the Deep Neural Network (DNN) to detect the IN location in the first stage and blank the detected IN signal in the second stage. The simulated results showed that the system can improve the performance since the DNN can learn from a huge number of examples and increase the accuracy of IN detection. In our paper, we further improve the performance of the conventional blanking scheme. Therefore, it is potential to combine the machine learning such as DNN and our proposed method to improve the performance.

On the other hand, Doppler shift is also one factor in degrading the performance due to mobile vehicles. Therefore, we need to investigate the performance of the proposed system in the mobile case. As we know, MIMO (Multiple Input and Multiple Output) can mitigate the BER performance and suppress the interference due to multiple antennas. Therefore, we can combine MIMO and the proposed system to improve the BER performance further.

Acknowledgements

Firstly, I would like to express my sincere gratitude to my supervisor Professor Minoru Okada, for the support of my research, for his patience and immense knowledge. I am thankful to Associate Professor Takeshi Higashino and Assistant Professor Duong Quang Thang, for providing valuable advices for my research. Also, I greatly appreciate Assistant Professor Na Chen and Assistant Professor Yafei Hou who guided and encouraged me in all the time of research. I thank all members of our lab for their discussions and advices about my research. And I am also thankful to Professor Kenji Sugimoto for his insightful comments.

Besides, I take this opportunity to thank Japanese Government who offered me the MEXT Scholarship Top Global University Project to mitigate my financial pressures. Thank for giving me the important scholarship to finish my doctoral research.

Finally, I would like to thank my family for always supporting me and encouraging me during my PhD research.

References

[1] Fourth Industrial Revolution from https://en.wikipedia.org/wiki/.

[2] D. Lukač, "The fourth ICT-based industrial revolution "Industry 4.0"- HMI and the case of CAE/CAD innovation with EPLAN P8," *2015 23rd Telecommunications Forum Telfor (TELFOR)*, Belgrade, pp. 835-838, 2015.

[3] S.I. Shafiq, C. Sanin, C. Toro and E. Szczerbicki, "Virtual engineering object (VEO): toward experience-based design and manufacturing for Industry 4.0," *Cybern. Syst.* vol. 46, no. 1-2, pp. 35-50, 2015.

[4] Y. Lu, "Industry 4.0: A Survey on Technologies, Applications and Open Research Issues," *Journal of Industrial Information Integration 6*, pp. 1-10, 2017.

[5] S. Wang, J. Wan, D. Li, and C. Zhang, "Implementing smart factory of industrie 4.0: An outlook," *Int. J. Distrib. Sensor Netw.*, vol. 12, no. 1, pp. 1-10, 2016.

[6] M. Ghobakhloo, "Industry 4.0, Digitization, and Opportunities for Sustainability," *Journal of Cleaner Production*, vol. 252, Apr., 2020.

[7] M. S. Carmo, S. Jardim, A. V. Neto, R. Aguiar and D. Corujo, "Towards fog-based slice-defined WLAN infrastructures to cope with future 5G use cases," *2017 IEEE 16th International Symposium on Network Computing and Applications (NCA)*, Cambridge, MA, pp. 1-5, 2017.

[8] J. F. Coll, "Channel Characterization and Wireless Communication Performance in Industrial Environments," Doctoral Thesis in Information and Communication Technology Stockholm, Sweden, Jun., 2014.

[9] A. Willig, K. Matheus and A. Wolisz, "Wireless Technology in Industrial Networks," in *Proceedings of the IEEE*, vol. 93, no. 6, pp. 1130-1151, Jun., 2005.

[10] Y. H. Ma, P. L. So and E. Gunawan, "Performance analysis of OFDM systems for broadband power line communications under impulsive noise and multipath effects," in *IEEE Transactions on Power Delivery*, vol. 20, no. 2, pp. 674-682, Apr., 2005.

[11] F. H. Juwono, Q. Guo, D. Huang and K. P. Wong, "Deep Clipping for Impulsive Noise Mitigation in OFDM-Based Power-Line Communications," in *IEEE Transactions on Power Delivery*, vol. 29, no. 3, pp. 1335-1343, Jun., 2014.

[12] L. M. H. Shhab, A. Rizaner, A. H. Ulusoy and H. Amca, "Impact of impulsive noise on millimeter wave cellular systems performance," *2017 10th UK-Europe-China Workshop on Millimetre Waves and Terahertz Technologies (UCMMT)*, Liverpool, pp. 1-4, 2017.

[13] M. Cheffena, "Industrial wireless communications over the millimeter wave spectrum: opportunities and challenges," in *IEEE Communications Magazine*, vol. 54, no. 9, pp. 66-72, Sept., 2016.

[14] P. Popovski, K. F. Trillingsgaard, O. Simeone and G. Durisi, "5G Wireless Network Slicing for eMBB, URLLC, and mMTC: A Communication-Theoretic View," in *IEEE Access*, vol. 6, pp. 55765-55779, 2018.

[15] G. Durisi, T. Koch and P. Popovski, "Toward massive, ultra reliable, and low-latency wireless communication with short packets," in *Proc. IEEE*, vol. 104, no. 9, pp. 1711–1726, 2016.

[16] F.B. Frederiksen and R. Prasad, "An overview of OFDM and related techniques towards development of future wireless multimedia communications," *Radio and Wireless Conference, 2002. RAWCON 2002. IEEE*, pp. 19-22, 2002.

[17] "FDM", https://en.wikipedia.org/wiki/Frequency-division-multiplexing.

[18] M. Takada and M. Saito, "Transmission System for ISDB-T," *Proceedings of the IEEE*, vol. 94, no.1, pp. 251-256, Jan., 2006.

[19] J. G. Andrews et al., "What will 5G be?," *IEEE J. Sel. Areas Commun.*, vol. 32, no. 6, pp. 1065-1082, Jun., 2014.

[20] A. Osseiran et al., "Scenarios for 5G mobile and wireless communications: the vision of the METIS project," in *IEEE Communications Magazine*, vol. 52, no. 5, pp. 26-35, May, 2014.

[21] T. S. Rappaport et al., "Millimeter Wave Mobile Communications for 5G Cellular: It Will Work!," in *IEEE Access*, vol. 1, pp. 335-349, 2013.

[22] M. Shafi et al., "5G: A Tutorial Overview of Standards, Trials, Challenges, Deployment, and Practice," in *IEEE Journal on Selected Areas in Communications*, vol. 35, no. 6, pp. 1201-1221, Jun., 2017.

[23] M. Ghosh, "Analysis of the effect of impulse noise on multicarrier and single carrier QAM systems," in *IEEE Transactions on Communications*, vol. 44, no. 2, pp. 145-147, Feb., 1996.

[24] K. Jamieson and H. Balakrishnan, "PPR: Partial packet recovery for wireless networks," in *ACM SIGCOMM*, 2007.

[25] D. Wang, Y. Cao and L. Zheng, "Efficient two-stage discrete bit-loading algorithms for OFDM systems," *IEEE Trans. Veh. Technol.*, vol. 59, no. 7, pp. 3407-3416, Sept., 2010.

[26] E. H. Choi, W. Choi, J. G. Andrews and B. F. Womack, "Power loading using order mapping in OFDM systems with limited feedback," *IEEE Signal Process. Lett.*, vol. 15, no. 5, pp. 545-548, Sept., 2008.

[27] A. Rahmati and P. Azmi, "Iterative reconstruction of oversampled OFDM signals over deep fading channels," in *Circuits and Systems for Communications, 2008. ECCSC 2008. 4th European Conference*, pp. 289-294, 2008.

[28] A. Rahmati, K. Raahemifar, T. A. Tsiftsis, A. Anpalagan and P. Azmi, "OFDM Signal Recovery in Deep Faded Erasure Channel," in *IEEE Access*, vol. 7, pp. 38798-38812, 2019.

[29] S. Takahashi, M. Hamamura and S. Tachikawa, "A demodulation complexity reduction method using M-algorithm for high compaction multi-carrier modulation systems," *1st International Symposium onWireless Communication Systems*, Mauritius, pp. 418-422, 2004.

[30] Erceg, V. L. Schumacher, P. Kyritsi, et al., TGn Channel Models, Version 4. IEEE 802.11-03/940r4, May, 2004.

[31] V. Fernandes, W.A. Finamore, M.V. Ribeiro, N. Marina and J. Karamachoski, "Bernoulli-Gaussian distribution with memory as a model for power line communication noise," in *Proc. Braz. Telecommun. Signal Process. Symp.*, 328–332, 2017.

[32] S.M. Curuk, "Impulsive Noise Models Used in Power Line Communications," *Balkan Journal of Electrical and Computer Engineering*, vol. 7, no. 2, pp.115–122, 2019.

[33] D. Middleton, "Statistical-physical models of electromagnetic interference," *IEEE Transactions on Electromagnetic Compatibility*, vol. 19, no. 3, pp. 106–127, Aug., 1977.

[34] T. Shongwey, A.J.H. Vinck, H.C. Ferreira, "On impulse noise and its models," *18th IEEE International Symposium on Power Line Communications and Its Applications*, Glasgow, pp. 12–17, 2014.

[35] S. V. Zhidkov, "Analysis and comparison of several simple impulsive noise mitigation schemes for OFDM receivers," in *IEEE Transactions on Communications*, vol. 56, no. 1, pp. 5-9, Jan., 2008.

[36] H. A. Suraweera, C. Chai, J. Shentu, J. Armstrong, "Analysis of impulse noise mitigation techniques for digital television systems," *Proc. 8th International OFDM Workshop*, pp. 172–176, 2003.

[37] S. V. Zhidkov, "Performance analysis and optimization of OFDM receiver with blanking nonlinearity in impulsive noise environment," in *IEEE Transactions on Vehicular Technology*, vol. 55, no. 1, pp. 234-242, Jan., 2006.

[38] U. Epple and M. Schnell, "Adaptive threshold optimization for a blanking nonlinearity in OFDM receivers," *2012 IEEE Global Communications Conference (GLOBECOM)*, Anaheim, CA, pp. 3661-3666, 2012.

[39] D. Tseng, Y. S. Han, W. H. Mow, L. Chang and A. J. H. Vinck, "Robust Clipping for OFDM Transmissions over Memoryless Impulsive Noise Channels," in *IEEE Communications Letters*, vol. 16, no. 7, pp. 1110-1113, Jul., 2012.

[40] T. Bai, H. Zhang, J. Zhang, C. Xu, A. F. A. Rawi, and L. Hanzo, "Impulsive noise mitigation in digital subscriber lines: The state-of-the-art and research opportunities," *IEEE Commun. Mag.*, vol. 57, no. 5, pp. 145–151, May, 2019.

[41] A. Al-Dweik, A. Hazmi, B. Sharif, and C. Tsimenidis, "Efficient interleaving technique for OFDM system over impulsive noise channels," in *Proceedings of IEEE PIMRC 2010*, pp. 167–171, Sep., 2010.

[42] S. Miyamoto, M. Katayama and N. Morinaga, "Performance analysis of QAM systems under class A impulsive noise environment," in *IEEE Transactions on Electromagnetic Compatibility*, vol. 37, no. 2, pp. 260-267, May, 1995.

[43] M. Skolnik, Introduction to Radar Systems. McGraw-Hill, 2000.

[44] S. Zahedpour, M. Ferdosizadeh, F. Marvasti, G. Mohimani and M. Babaie-Zadeh, "A novel impulsive noise cancellation based on successive approximations," in *Proceedings of SampTa 2007*, pp. 126–131, 2007.

[45] S. Zahedpour, S. Feizi, A. Amini, M. Ferdosizadeh and F. Marvasti, "Impulsive Noise Cancellation Based on Soft Decision and Recursion," in *IEEE Transactions on Instrumentation and Measurement*, vol. 58, no. 8, pp. 2780-2790, Aug., 2009.

[46] Y. F. Hou and M. Hamamura, "Collision recovery for OFDM system over wireless channel," *IEICE Trans. on Fundamentals*, vol. E90-A, no. 7, pp. 1312-1322, Jul., 2007.

[47] Y. F. Hou and T. Hase, "Collision-recovery method for collided OFDM based packets," *2008 IEEE 19th International Symposium on Personal, Indoor and Mobile Radio Communications*, Cannes, pp. 1-6, 2008.

[48] R. Barazideh, S. Niknam, and B. Natarajan, "Impulsive noise detection in OFDM-based system: A deep learning perspective," in *IEEE Comput. Commun. Work. Conf. (CCWC)*, pp. 937–942, Jan. 2019.

Publication List

Journal

[1] Chengbo Liu, Na Chen, Minoru Okada and Yafei Hou, “SMLB based OFDM receiver over impulsive noise environment”, *APSIPA Trans. on Signal and Information Processing*, vol. 9, e23, pp. 1-8, 2020.

International Conference

[1] Chengbo Liu, Yafei Hou, Takeshi Higashino and Minoru Okada, “A proposal of half-symbol parallel combinatory multicarrier modulation for one-seg service of ISDB-T system”, In Proc. *International Symposium on Broadband Multimedia Systems and Broadcasting (BMSB 2016)*, pp. 1-4, Jun. 2016.

[2] Chengbo Liu, Yafei Hou, Takeshi Higashino and Minoru Okada, “Orthogonal parallel combinatory amplitude shift keying modulated multicarrier system”, In Proc. *International Symposium on Communications and Information Technologies (ISCIT 2016)*, pp. 7-10, Sept. 2016.

[3] Chengbo Liu, Na Chen, Minoru Okada and Yafei Hou, “Time-Domain Signal Recovery for OFDM System in the Industrial Environment”, *2019 Asia-Pacific Signal and Information Processing Association Annual Summit and Conference (APSIPA ASC)*, pp. 1847-1851, Lanzhou, China, 2019.